Upper Quaternary deposits on the Sao Tomé deep-sea channel levee system (South Brazilian Basin): major turbidite versus contourite processes

E. Gonthier [a,*], J.-C. Faugères [a], A. Viana [b], A. Figueiredo [c], P. Anschutz [a]

[a] Département de Géologie et Océanographie, UMR 5805 'EPOC', Université Bordeaux I, Talence 33405, France
[b] Petroleo Brasileiro S.A., Avenida Elias Agostinho 665, Macae, RJ 27913-350, Brazil
[c] Laboratorio de Geologia Marinha, Instituto de Geociencias, Universidade Federal Fluminense, Avenida Litoranea, 24210-340 Niteroi, RJ, Brazil

Abstract

This paper is an attempt to show how one may discriminate turbiditic and contouritic processes in the deposition of deep-sea accumulations. The case study is the Sao Tomé deep-sea 'channel levee' system in the South Brazilian Basin. This system is elongated parallel to the margin contour, and was first interpreted as being controlled by contour current activity. Detailed analyses of 3.5-kHz profiles and piston cores allowed to demonstrate that the Upper Quaternary sediments are predominantly deposited by turbidite and hemipelagic–pelagic sedimentation processes. On the levee and the transitional area towards the deeper rise, frequent fine-grained turbidites, accounting for 25–45% of the entire depositional series, are interbedded with the hemipelagic–pelagic muds. In the channel, thicker and coarser turbidites (15%) are associated with debris-flows (20%). Deposit deformation in the form of slides, slumps and diapir-like structures largely affect the distal transitional area. Slight evidence of contour current activity only consists of some sediment wave fields and manganiferous-rich layers or some top-truncated sequences and foraminiferal sandy layers.
© 2003 Elsevier Science B.V. All rights reserved.

Keywords: Brazilian Basin; channel levee system; Echo-facies; Turbidite; Contourite; Upper Quaternary

1. Introduction

Major processes of building of deep-sea sedimentary levees, associated with turbidite 'channel levee' and contourite 'moat drift' systems, are difficult to assess from depositional geometry alone. This is because these two types of levee may have similar patterns such as a trend with respect to the margin, internal deposit geometry and bedforms (i.e. McCave and Tucholke, 1986; Faugères et al., 1999). It is still more difficult when the turbidite and contourite processes interact within the sediment deposition.

* Corresponding author. Tel.: +33 0540-00-88-33;
Fax: +33 0540-00-88-48.
  E-mail address: egonthier@epoc.u-bordeaux1.fr
(E. Gonthier).

The purpose of this paper is to show how one may discriminate both processes from an example of such a scenario that is frequent in the deep-sea. The case study is located in the South Brazilian Basin where a gently mounded sedimentary accumulation, called the Sao Tomé 'channel levee' system (Viana, 1998), is deposited on the continental rise.

The Sao Tomé system (Figs. 1 and 2) is elongated N–S, more or less parallel to the margin contour. The area is swept by two water masses, the North Atlantic Deep Water (NADW) and the Antarctic Bottom Water (AABW). Because of this morphological and hydrological background, the system was first interpreted as a moat drift system (Mello et al., 1992). The aim of the study is to demonstrate that the processes involved in the Sao Tomé system deposition, during the Upper Quaternary, were controlled by major turbidite and pelagic-hemipelagic processes, and contourite processes. Such an interpretation is supported by the analysis of the system physiography and the deposit distribution. It is consistent with that proposed for the Cenozoic deposits by Viana et al. (2003).

2. Data collection and methods

The study is based upon 500 km of 3.5-kHz lines, and 7 Kullenberg cores (Fig. 3a; Table 1), collected from most of the environments recognized in the system (Faugères, 1988). The 3.5-kHz lines were interpreted using the echofacies types defined by Damuth and Hayes (1977), Damuth (1980), Jacobi (1982), and Mézerais et al. (1993). The cores were described in detail and underwent the following analyses: (1) the sedimentary structures were identified using digital radiography images (SCOPIX, Migeon et al., 1999); (2) components were identified from smear slides (semi-quantitative analyses); (3) the total percentage of carbonates was determined (gasometric method); (4) grain-size was determined based on a laser microsizer, Malvern Mastersizer Ls, and statistical analysis of grain size parame-
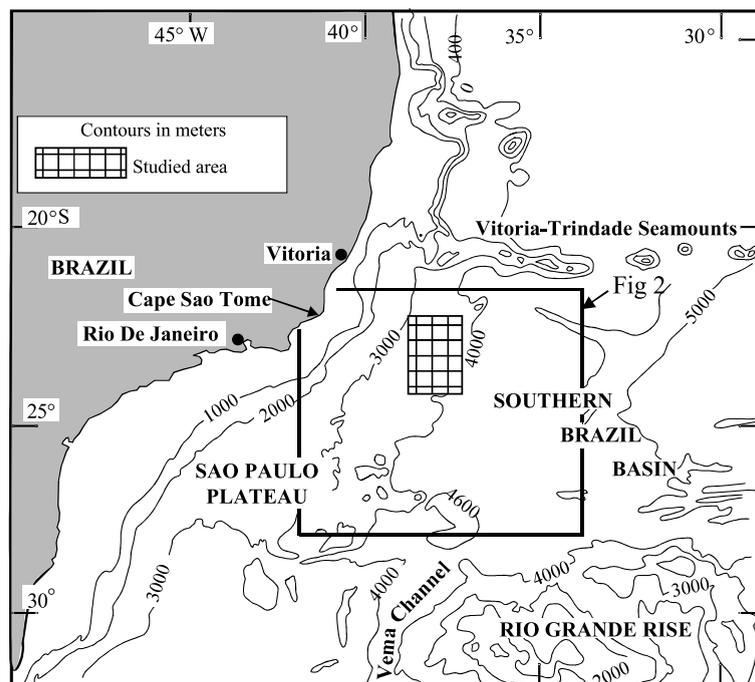

Fig. 1. Atlantic Ocean offshore Brazil with outline of the study area, and location of Fig. 2.

ters (mean, median, percentage of particles > 63 μm, percentage of particles between 63 and 10 μm, percentage of particles < 10 μm, sorting); (5) mineralogical analyses were made by X-ray diffractometry (light minerals and clay minerals studied on the decarbonated fraction below 2 μm; method of oriented deposits, Latouche and Maillet, 1984); and (6) geochemical analyses were made of the dark laminated muddy layers observed in the cores. The organic carbon content was first measured, using a Leco CIS analyzer, after decarbonation of the dry samples. Then leaching of the sediments was performed using a solution of 1N HCl that can dissolve Fe and Mn associated with oxides or carbonates. Fe and Mn were analyzed by flame atomic absorption from the filtered 1N HCl solution, after 24 h of leaching.

According to a preliminary stratigraphical study (J. Duprat, pers. commun., 2002), these cores represent the Upper Quaternary (the last 400 000 years as an average).

3. Morphological and hydrological background

The South Brazilian Basin continental margin (Figs. 1 and 2) includes a large plateau, the Sao Paulo Plateau (SPP), located on the continental slope at a depth of about 2000–3400 m. The SPP is bounded downslope by a slope break, the SPP Escarpment (SPPE), about 200 m high, that shows an irregular trend more or less parallel to the trend of the margin (Figs. 2 and 3b). Beyond the SPPE, the upper rise presents a fairly irregular surface that gently slopes down towards the abyssal plain. A complex network of channels crosses the SPP (Fig. 2), and then converges downslope into a small number of large and shallow major channels that run across the rise (Brehme, 1984;
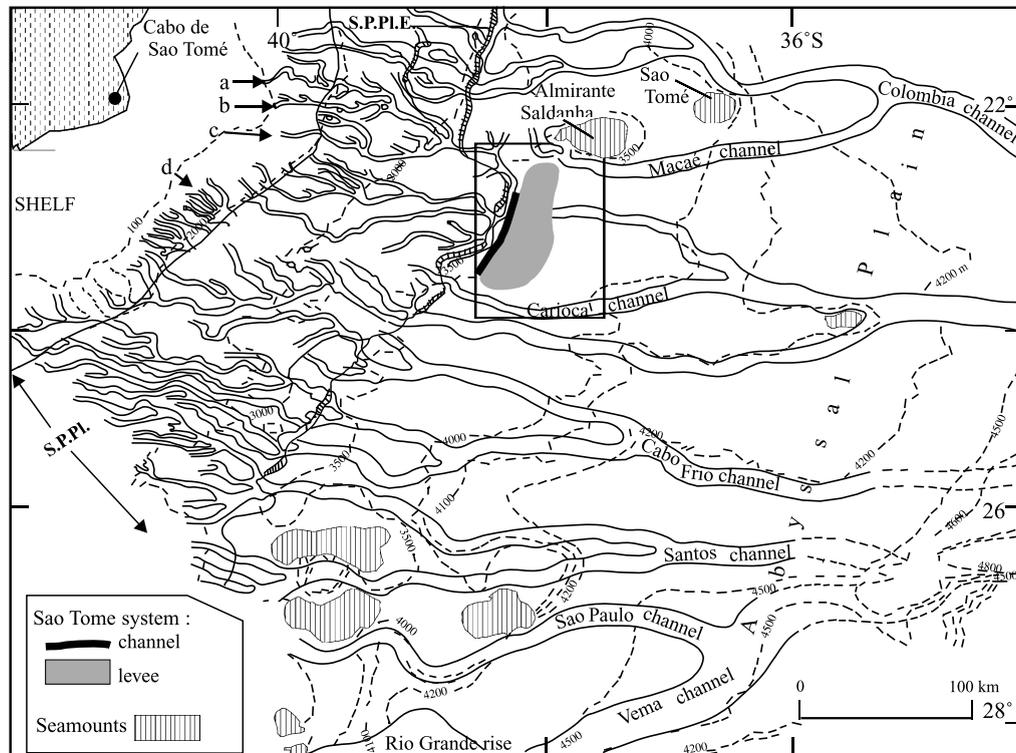

Fig. 2. Physiography of the South Brazilian continental margin and channel network (from Castro, 1992). Key: (a) Almirante Camara canyon; (b) Itapimiri canyon; (c) Sao Tomé canyon; (d) Sul Este canyon; S.P.Pl., Sao Paulo Plateau; S.P.Pl.E, Sao Paulo Plateau escarpment. Outlined area indicates the area of study.

Mello, 1988; Castro, 1992; Miller et al., 1996). However, the available bathymetric data are insufficient to show reliable connections between most of the SPP channels and channels on the rise.

The Sao Tomé 'channel levee' system (Figs. 3 and 4), about 100 km long and 60 km large, is elongated at the foot of the northern part of the SPPE, about 22–24°S. It comprises a gently mounded levee that is separated from the escarpment by a N–S directed trough called the Guanabara channel, at a water depth ranging from 3500 to 4000 m. Such a depth corresponds today to the transitional zone between the NADW and the AABW (Reid et al., 1977). The NADW flows southward at a depth ranging from 1200 to 3500–4000 m with a very low velocity (less of 5 cm/s), while the AABW flows northward at a depth greater than 4000 m with a velocity that does not exceed 10 cm/s in the open basin. However, recent data (e.g. Reid, 1989, 1996; DeMadron and Weatherly, 1994; Siedler et al., 1996; Hogg et al., 1996; Hogg and Zenk, 1997; Muller et al., 1997) have shown a far more complex modern circulation, revealing episodes of opposite directional trend and/or higher velocity for both circulation patterns. Uncertainty of the Quaternary paleocirculations is even greater (Massé et al., 1994; Siedler et al., 1996). As a consequence of this hydrological background, the sediments on the south Brazilian rise were considered as mainly controlled by the AABW currents (Damuth and Hayes, 1977; Gamboa et al., 1983; Mello et al., 1992; Castro, 1992; Mézerais et al., 1993; Massé et al., 1996; Petchick et al., 1996), and the levee, elongated parallel to the Guanabara channel, was interpreted as a drift (Mello et al., 1992).

4. Physiography of the Sao Tomé 'channel levee' system

An improved bathymetric map of the Sao Tomé 'channel levee' system (Fig. 3) was constructed that shows the different depositional areas and associated channels. The system is composed of three major sedimentary domains oriented N–S: (1) the Guanabara channel, (2) an area of maximum deposition along the eastern flank of the channel, called the levee (s.s.), and (3) a transitional area between the levee and the lower rise seaward.

The Guanabara channel (Figs. 3–5) is about 70 km long, with a width that ranges from 2 km in the north, to 10 km in its central part and 4 km in the south. Its depth is about 200 m with respect to the top of SPPE. It is up to 75 m deep in its mid-part with respect to the levee, and it narrows progressively north and southward. This channel seems then to close at both ends with a slightly sinuous course. The channel bottom is fairly flat with a few low mounded reliefs (1 km or more long and about 15 m high) that could result from erosive residual relief or slide and debris-flow deposits (Fig. 5c).

The levee (s.s.) is 60 km long and up to 30 km wide, more or less elongated in N–S direction. It is formed by two sedimentary elevations, one in the north and the other one in the south, separated by an E–W running central depression in the middle part of the system (Fig. 3b). The depression is about 30 km in diameter and 40 m deep, and opens eastward towards the deep basin. It seems to represent a major slope failure that crosses the transitional area. Secondary N–S to E–W directed channels converge towards the eastward sloping axis of the depression.

In the north (Figs. 3, 4a,b, 5a and 6e), the levee presents an asymmetrical mounded shape with a short flank towards the channel and a widespread eastern flank gently sloping basinward. It widens and the levee crest deepens southward (Figs. 3b and 5). The seafloor shows large flat areas with a few small-sized bulge-like features scattered throughout (Figs. 4 and 5d). In the south (Figs. 3 and 4c,d), the levee has the shallowest depth (3500 m) and shows a more symmetrical shape and a seafloor surface molded by either small-size sediment reliefs or wavy bedforms. It deepens towards the central part of the levee further north.

The transitional zone (Figs. 3, 4 and 7) presents a more irregular seafloor. The boundary with the levee may be marked by a low relief escarpment (Fig. 4, F1 minor fault). In the north and the middle part of the system (Fig. 7), there are hum-
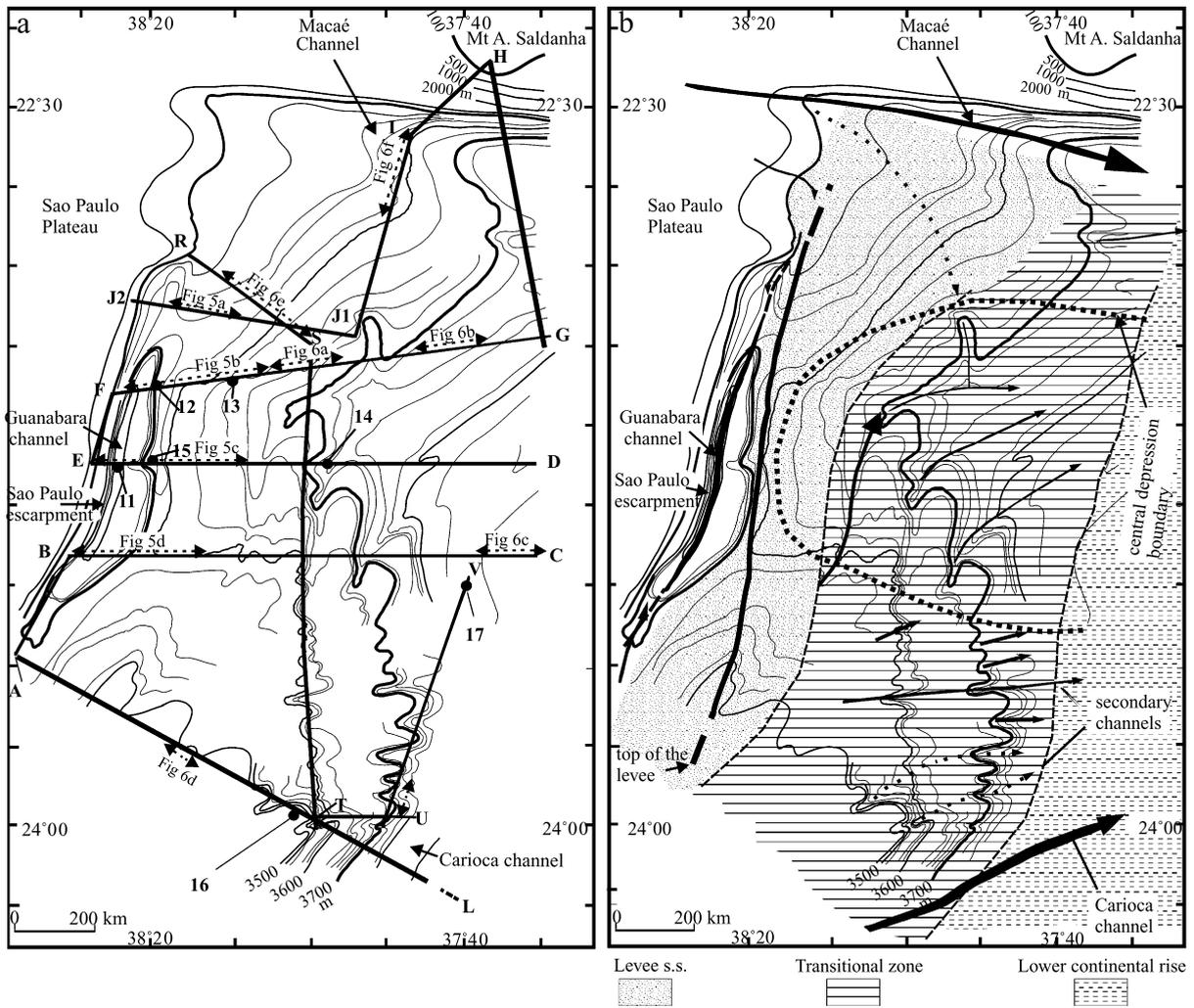
Fig. 3. Detailed bathymetric map of the Sao Tomé channel levee system. (a) Location of cores (numbered 11–17) and 3.5-kHz seismic lines; dashed lines indicate the length of the seismic lines covered by the seismic lines presented in Figs. 5 and 6. (b) Depositional areas and associated channels (arrows suggest turbidity current pathways).

mocky or wavy bedforms and other minor sediment reliefs (bulges or diapir-like structures) associated with small-sized depositional depressions or elongated troughs (secondary channels?). These features have mostly a WSW–ENE trend, and could be initiated by post-depositional sediment deformation, and then eroded by turbidity or bottom currents. Eastward (Fig. 6b,c), the relief is mostly due to deposit sliding or slumping (compressional ridges, hummocky bedforms) associated with diapirs. In the south, the seafloor mor-

phology is more regular (Figs. 3 and 4d), with wavy bedforms (Fig. 6d) and W–E directed gullies (Fig. 3).

Two major shallow channels (15–20 km wide and 40–60 m deep), bounding the study area in the north and the south (Fig. 3), may be involved in sediment supply to the system. The Macaé channel in the north (Figs. 2, 3 and 6f) is connected upslope with the northern Campos Basin canyons on the upper slope (Viana, 1998) and the channel network that runs across the SPP (Ma-

Table 1
Core location

Core number	Pilote number	Latitude	Longitude	Depth (m)	Length (m)	Environment
KS 8811		23°14′39″	38°27′20″	3650	5.60	Channel
KS 8812		23°05′57″	38°19′05″	3580	8.00	Levee top
KS 8813		23°06′36″	38°09′34″	3635	6.38	Levee E flank
KS 8814		23°14′23″	37°56′58″	3660	4.24	Transitional zone
KS 8815		23°15′02″	38°19′66″	3590	4.50	Levee top
KS 8816		23°59′96″	38°00′20″	3530	5.97	Transitional zone
KS 8817		23°30′09″	37°40′09″	3834	5.64	Continental rise
	USN 8803	23°30′02″	37°39′78″	3835	0.38	Continental rise

chado et al., 1997; Gorini et al., 1998), and down-slope with the Columbia channel that lies to the northeast (Brehme, 1984, and pers. commun., 2001). It should play a major role in feeding the northern part of the system. The Carioca channel in the south (Figs. 2 and 3) is known from published and unpublished data (Brehme, 1984; Mello, 1988; Castro, 1992; Alvés, 1999; and I. Brehme, pers. commun., 2001) to cross the rise close to the southern end of the studied area. As it is only crossed by one of our profiles (southeast corner of the mapped area; Fig. 4d), it is difficult to unravel the exact role of this channel in the levee construction. However, we suspect that it should be responsible for both the erosional and depositional processes, at least in the southern area. The linkage between the channel and the upper margin drainage system remains unclear (Viana, 1998).

5. Deposit pattern

The surficial deposits show a large variability of 3.5-kHz echo and sediment facies. The echofacies characteristics will be described first, followed, in more detail, by the depositional facies and vertical organisation, together with the distribution at the scale of the entire system, in order to point out the major processes involved in the sediment deposition.

5.1. Echofacies

The surficial sediments are illustrated in Figs.

5–7, and their distribution is shown in Fig. 8. Six major echofacies types have been defined. Their interpretation is based on the literature and core collected in the area.

Echofacies IIB, prolonged echo without sub-bottom reflectors, covers the seafloor of the channels encountered in the studied area, except in most of Guanabara channel. It characterizes environments of highest energy and active sediment transport like Macaé channel, Carioca channel and some other secondary channels (Figs. 5a, 6f and 7b). Echofacies IIA, more or less prolonged echo with discontinuous subbottom reflectors, occurs on most of Guanabara channel seafloor and the adjacent flank of the levee (Figs. 5 and 7b), and characterizes an environment of fairly high energy (see core 11). Echofacies IIA–IB (Figs. 5–7), sharp to semi-prolonged echo with continuous to discontinuous subbottom reflectors, covers most of the levee and the transitional zone. It corresponds to low-energy turbidite overflowing processes and pelagic-hemipelagic sedimentation (see cores 15, 12, 13 and 14). Two sub-echofacies have been defined in order to distinguish deposits either more or less undulating and covering flat areas, or horizontal and filling up small depressions (echo IIA–IB1, i.e. Figs. 5a and 6e), and deposits draping mounded small reliefs (IIA–IB2, i.e. Fig. 5d). Echofacies IIIF (Fig. 6d) is a regular wavy echo with continuous to discontinuous reflectors. It mainly occurs in the southern part of the levee where it shows continuous subbottom reflectors and a high penetration (25–30 m). It is interpreted as fine-grained sediments forming depositional sediment waves of possible
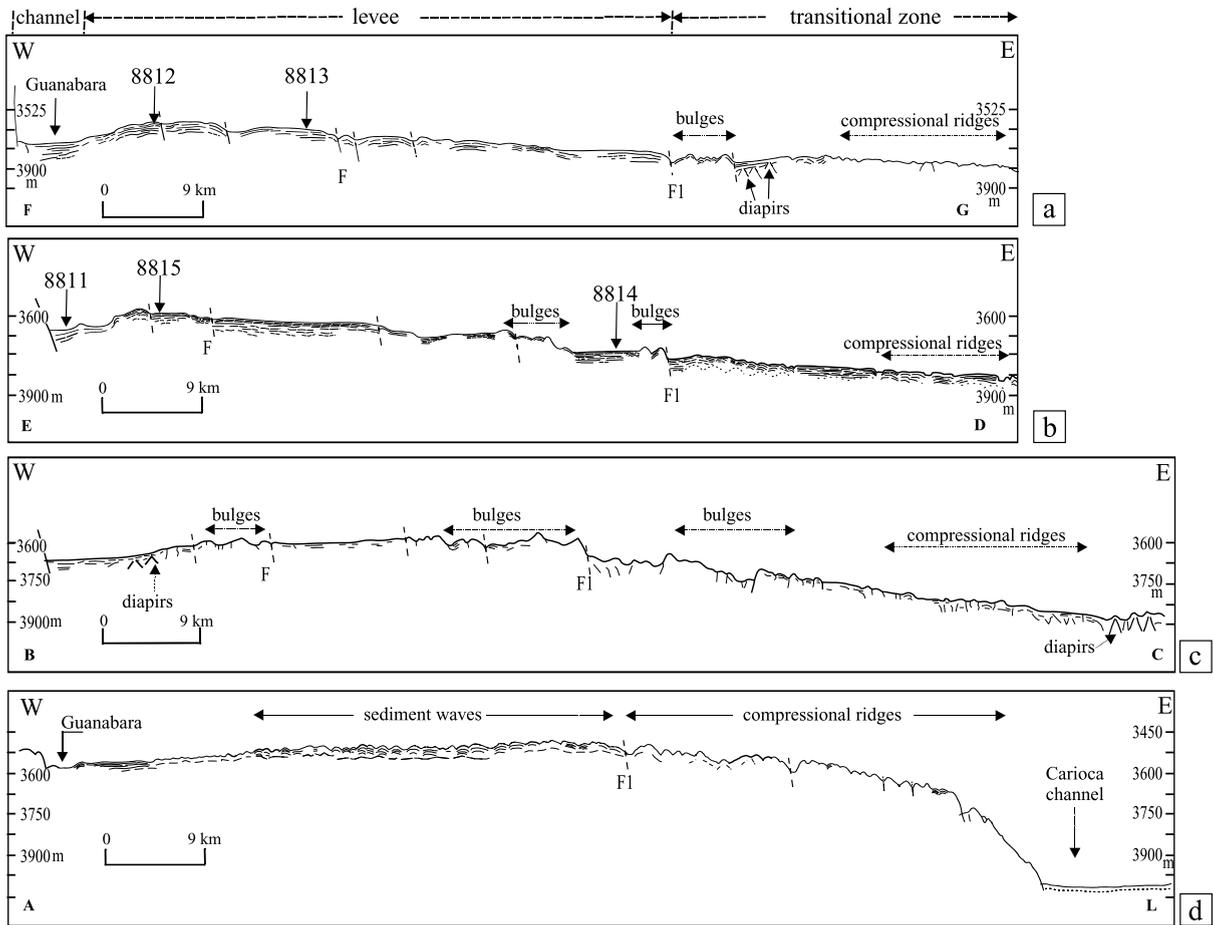
Fig. 4. Bathymetric profiles crossing the the Sao Tomé channel levee system and location of cores KS8811–KS8815. (a) Northern part (profile FG). (b) Northern central part (profile ED). (c) Southern central part (profile BC). (d) Southern part (profile AL). See Fig. 3a for profile location. Key: F, mini-faults; F1, mini-fault that marks the boundary between the levee and the transitional zone.

contour current origin (cf. Section 7). No core has been collected in this region. Echofacies IIIB (Figs. 6c and 7c), irregularly undulating semi-prolonged echo with continuous to discontinuous reflectors, is located along the deepest part of the transitional zone in the central depression (core 17, below). It could be interpreted as mudwaves, or because it is frequently associated with possible intrusive structures showing transparent echofacies (mud diapirs?) as the result of post-depositional gravity deformations like creeping, sliding or slumping, associated with compressional ridges. Echofacies IIIC (Figs. 6b and 7c), showing large hyperbolae with various elevations, could

also represent deposits that are more highly disturbed by mass transport associated with hummocky bedforms or compressional ridges. It is well-developed in the southeastern part of the system.

5.2. Sedimentary facies

The deposits are mostly fine-grained with variable carbonate contents (0–60%). Sandy–silty layers appear in the form of thin beds (commonly millimeter- to centimeter- and more rarely decimeter-thick, up to 3 dm) associated with turbidite sequences. They never represent more than 29%
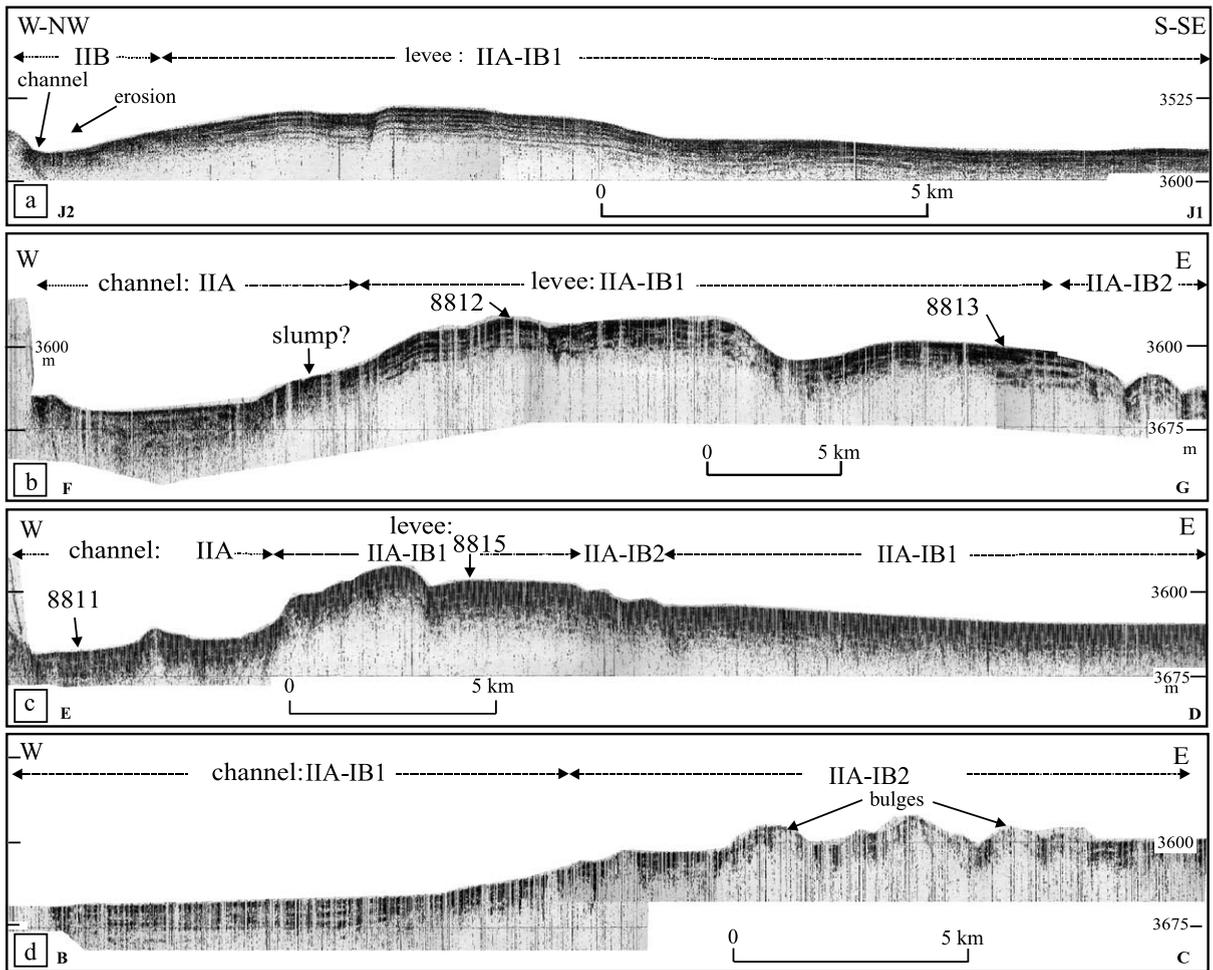
Fig. 5. North–south evolution of the Guanabara channel and adjacent levee. (a) Detail of profile J2J1. (b) Detail of profile FG. (c) Detail of profile ED. (d) Detail of profile BC. See Fig. 3 for profile location.

of the studied cores. Four facies have been defined according to the sediment grain size: the muds, silty–clayey (silt fraction < 30%) or clayey–silty (silts = 30–50%); the silts (silt fraction > 50%, sand fraction < 30%, mean diameter = 10–50 μm); the silty sands (sand fraction > 30%, mean diameter = 55–70 μm, 140 μm exceptionally).

The muds are called calcareous muds when the carbonate content exceeds 30%, and slightly calcareous muds when the carbonate content ranges from 15 to 30%.

The siliciclastic silty sand is composed of major quartz associated with minor feldspars, and heavy minerals. Preliminary analyses of clay mineral as-semblages show predominantly illites (30–65%) and kaolinite (20–40%) with minor smectite (15–20%) and chlorite (10–20%). A significant content of kaolinite reflects the influence of continental material supply (Chamley, 1975; Mello et al., 1992; Massé et al., 1996). Chlorite content never exceeds 20%. However the highest chlorite values (15–20%) could be evidence of material trans-ported from high latitudes by the AABW contour currents (Biscaye, 1965; Massé et al., 1996). The biogenic fraction contains abundant planktic fo-raminifera associated with shell debris, nannofos-sils and fairly rare benthic foraminifera. Siliceous biogenic debris (diatoms mainly) and abundant
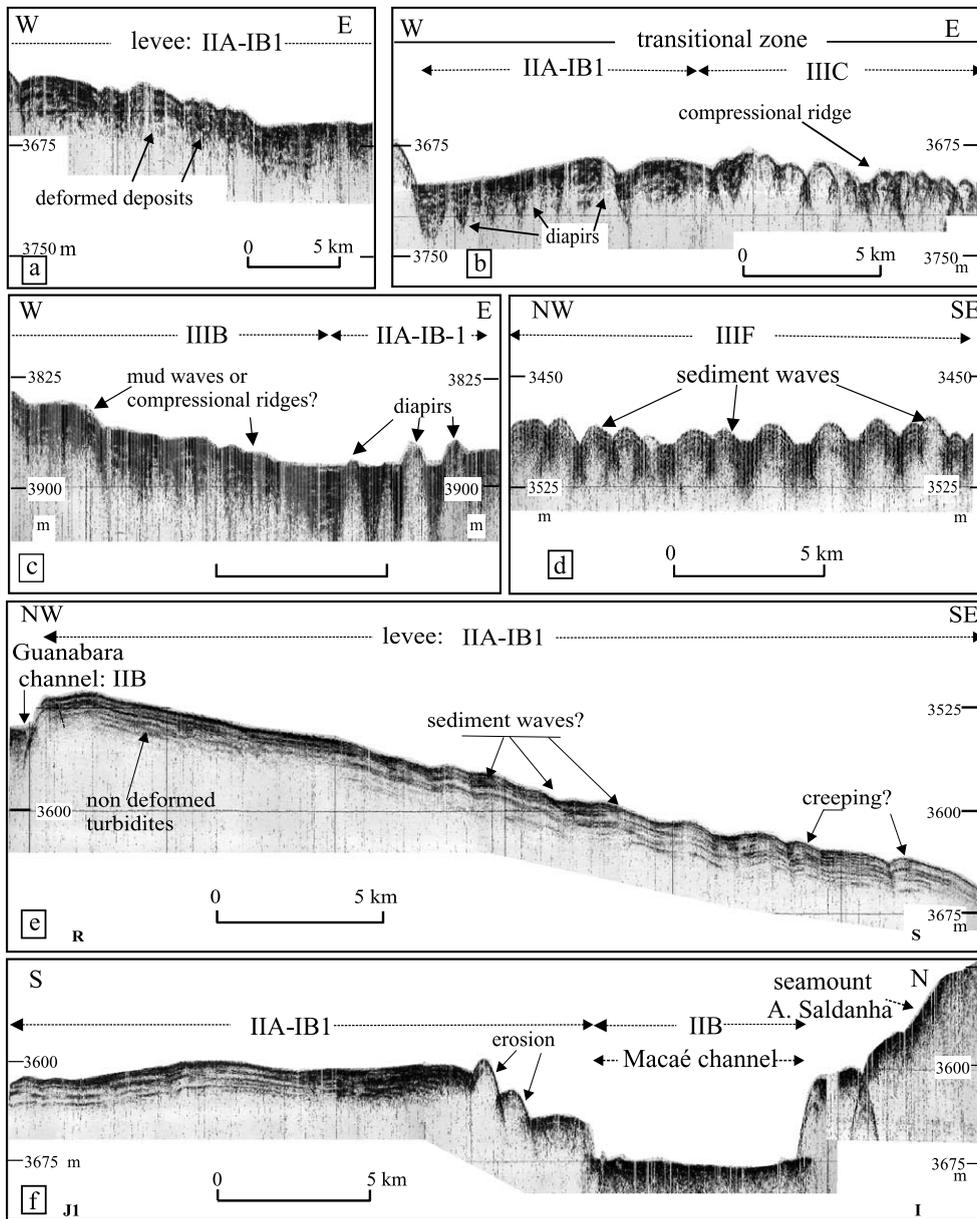
Fig. 6. Details of the 3.5-kHz profiles crossing the Sao Tomé channel levee system (see Fig. 3a for profile location): echofacies and bedform interpretation. (a) Deformed deposits (profile FG). (b) Slide and diapir-like structures (profile FG). (c) Diapir structures (profile BC). (d) Very regular wavy bedforms interpreted as depositional sediment waves (profile LA). (e) Deposits affected by creeping or gentle sliding (profile RS). (f) J1I profile crossing Macaé channel, and showing IIB echofacies in the Macaé channel seafloor, and erosion on the channel flanks suggesting active channels. Note the fairly continuous reflections with decreasing deposit thickness southward, and possible downlapping geometry, suggesting turbidity current overflowing processes of deposition.
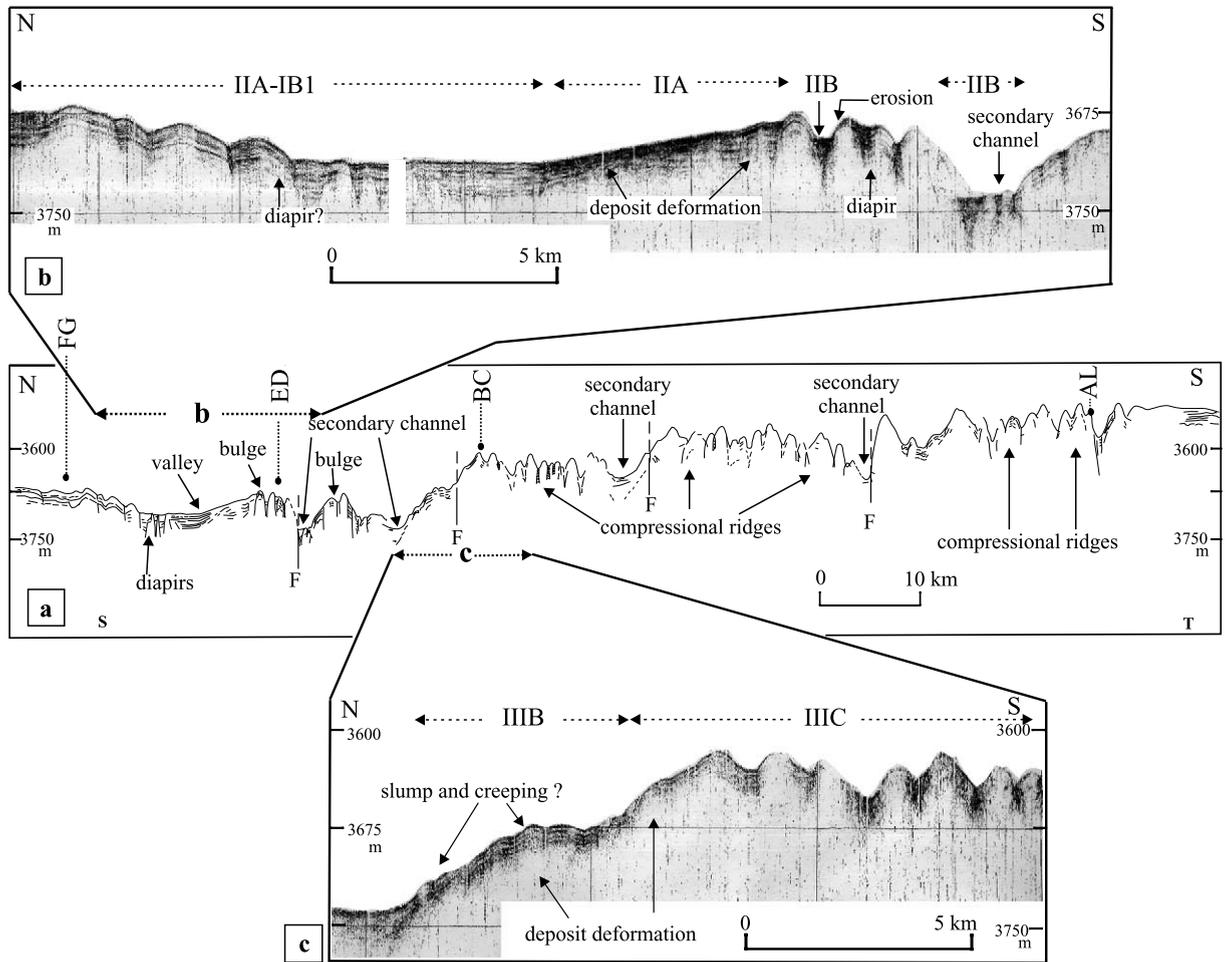
Fig. 7. N–S 3.5-kHz profile ST crossing the Sao Tomé channel levee system (see Fig. 3 for profile location). (a) Profile ST (crossing with profiles FG, ED, BC, and LA are indicated). Key: F, mini fault. (b,c) Details of the associated 3.5-kHz echofacies.

pteropod shells may be observed in some muddy beds. Authigenic manganiferous micronodules are frequently observed in the pelagic calcareous muds.

In addition to these major siliciclastic facies, two others are observed: calcareous foram-rich sands that are very rare and form thin centimeter-thick layers, and manganiferous clayey–silty muds that occur more frequently in some cores than in others.

5.3. Sedimentary sequences

The facies are vertically organized in sequences that reflect the depositional processes.

5.3.1. Hemipelagic and pelagic sequences

They are composed of greenish carbonate-free or slightly calcareous silty–clayey to clayey–silty muds, interpreted as hemipelagic deposits, overlain by brownish yellow calcareous silty–clayey to clayey–silty muds, interpreted as pelagic deposits. Cycles of pelagites and hemipelagites of climatic origin may be observed. They form beds of variable thickness (centimeter to decimeter). Sometimes carbonate-free or slightly calcareous mud layers are sandwiched between turbidite sequences. They are interpreted as hemipelagic deposits when there is no evidence of any graded bedding. Otherwise, they are considered as
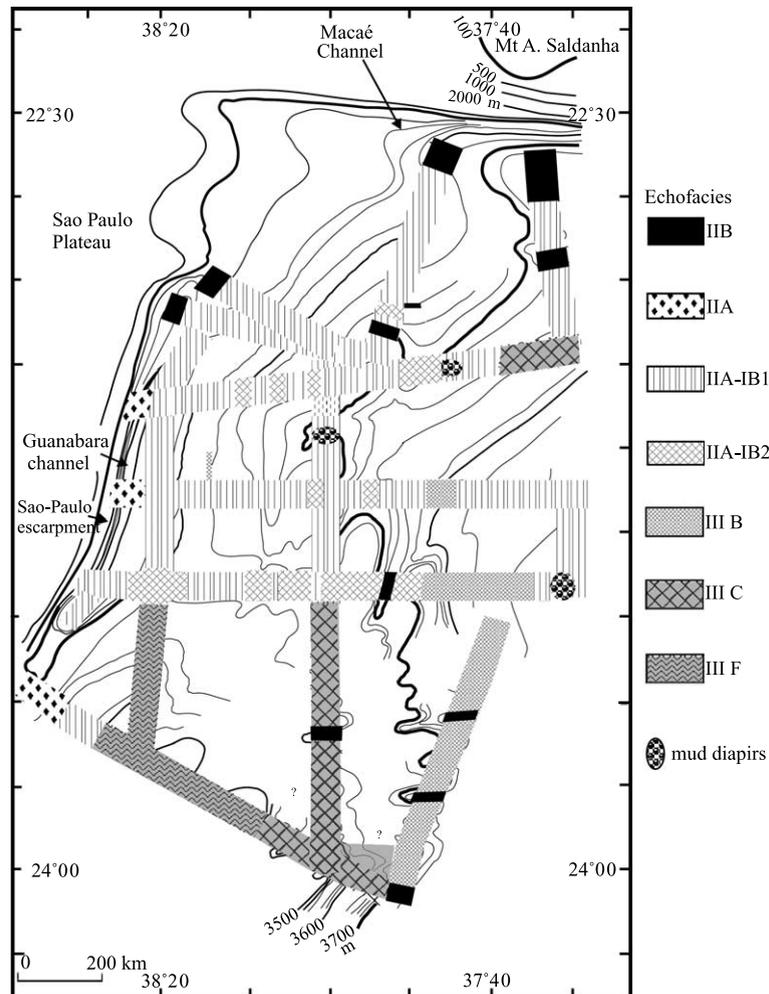
Fig. 8. Echofacies distribution on the Sao Tomé channel levee system. Key: IIB, continuous, sharp prolonged echoes, or discrete hyperbolae; IIA, discontinuous subbottom reflector; IIA–IB1, discontinuous or continuous subbottom reflector; IIA–IB2, discontinuous or continuous subbottom reflector, shaping residual relief; IIIB, irregularly ondulated with continuous to discontinuous parallel subbottom reflector: compressional ridges or sediment waves (?); IIIC, large hyperbolae, with various elevation: hummocky bedforms and compressional ridges; IIIF, regularly undulating with subbottom reflector: sediment waves (?).

part of the Bouma sequences (Td muddy division).

5.3.2. Turbidite sequences

The turbidite sequences (Fig. 9) display variations in thickness, grain size, and composition.

The *T1 turbidite sequence* corresponds to a thin-bedded (a few centimeters to 2 dm), graded, fine-grained four-division sequence. It is comprised of a very thin (2–10 cm) silt basal layer (mean diameter 15–25 μm), overlain by a succession of silty then clayey–silty and finally silty–clayey layers (mean diameter down to 5 μm). The three uppermost divisions may be either homogenous (type T1-a) or with sedimentary structures such as tiny laminations (type T1-l) or alternating clayey–silty and silty–clayey beds (a few millimeters to centimeters thick), decreasing in thickness and grain size upward (type T1-b). This T1 type corresponds to turbidity currents of low to very low density, and the T1-b type is often deposited by turbidity currents overflowing a levee
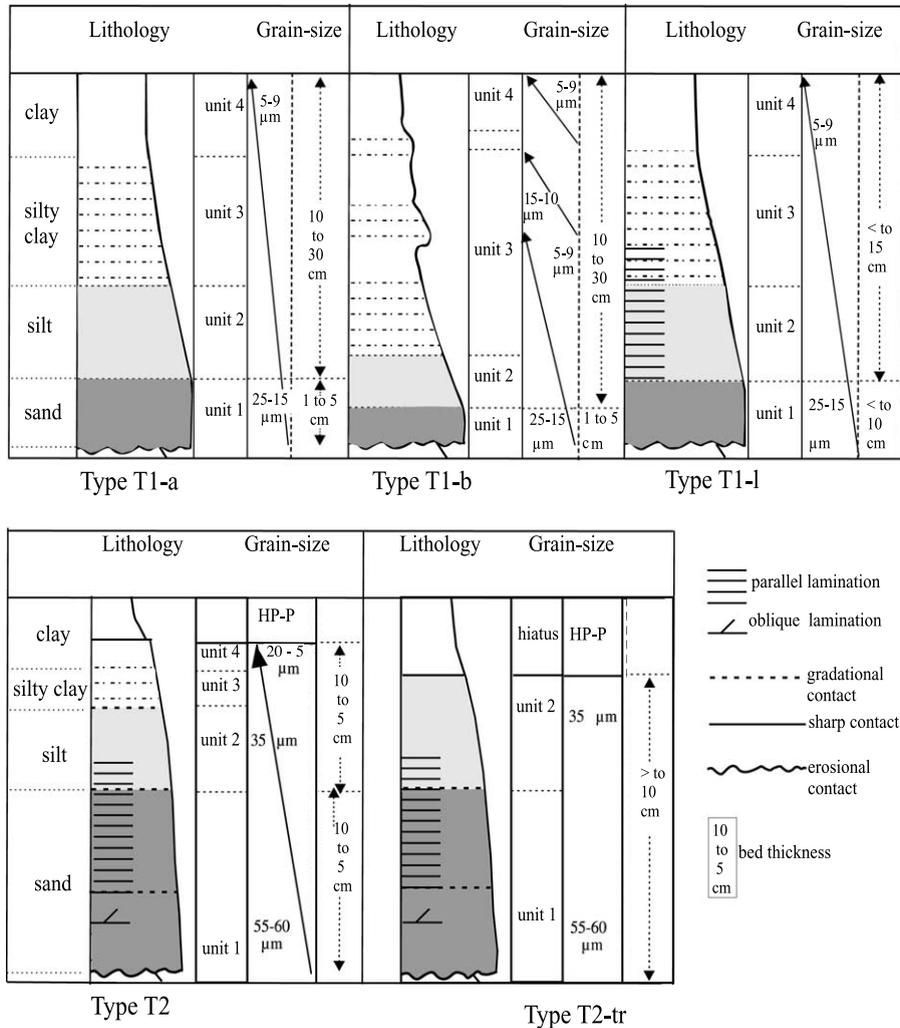
Fig. 9. Schemes of the main types of turbiditic sequences (T1 and T2, turbiditic sequence types).

(Hiscott et al., 1997; Migeon et al., 2001; Gervais et al., 2001).

The *T2 turbidite sequence* differs from the T1 type by having a coarser-grained (mean diameter of 35–140 μm), a thicker (10–15 cm) basal silty–sandy layer, and a thinner upper silty–clayey division. It may occur either as a four-division positive graded sequence (type T2), or as a top-truncated two-division sequence, with a sharp upper limit (type T2-tr). Such sequences are deposited by turbidity currents of higher density and velocity. The T2-tr sequence may be the result of a bypassing process or a contour current reworking process.

In addition, debris-flow sequences may be associated with T2 coarse-grained turbidites as in the Guanabara channel. Some other disturbed deposits (debris-flows or minor slump?) are rarely interbedded in deposits of the levee or transitional area (see below).

5.3.3. Peculiar sedimentary sequences

Two types of peculiar sequences display features that suggest deposition that could be controlled by contour currents.

The *Foram-rich sandy sequence* (F-sequence) is very rare (only two examples, in cores 12 and 13) and appears as a thin (5 cm) calcareous foram-

rich sandy layer, interbedded in hemipelagic–pelagic deposits. It is composed of predominantly planktonic foraminifera (70–80% carbonate), and minor siliciclastic grains, with a mean diameter of about 180 μm for the bulk sediment and 15 μm for the siliciclastic fraction. It shows sharp to erosional basal and upper limits. There is neither a clear graded bedding nor very good sorting of the grains. Such a sequence could be top-truncated turbidites with only the deposition of the basal layer in which the foraminifera have been concentrated, as we have observed high foraminifer contents (20–40%) in some T2 turbidite basal layers. However, the absence of graded bedding strongly suggests deposition under bottom currents that winnow pelagic deposits.

Examples of the *Manganiferous silty–clayey sequence* (Mn-sequence; Fig. 10) are muddy and appear at the top of turbidite sequences or inter-bedded in hemipelagic–pelagic deposits. They form a 3–10-cm-thick layer showing darkish to brownish millimeter-thick laminations with black micronodules, alternating with greenish–yellow hemipelagic–pelagic muds. Erosional surfaces are frequently observed inside and at the top or the base of the sequences. The black micronodules are interpreted as Mn-nodules oxides. The origin of the black color was tested using different chemical leaching. The results showed that the C-org content was always lower than 0.3%. No characteristic smell of H2S during the leaching with a 1N HCL solution was observed, attesting that the dark color was not due to iron monosulfides; the sediments were enriched in Mn and Fe (Mn: 1100–4300 ppm instead of about 300–800 ppm in the pelagic-hemipelagic muds; Fig. 10).

Two origins may be considered for such Mn-rich layers. Firstly, a diagenetic origin with Mn
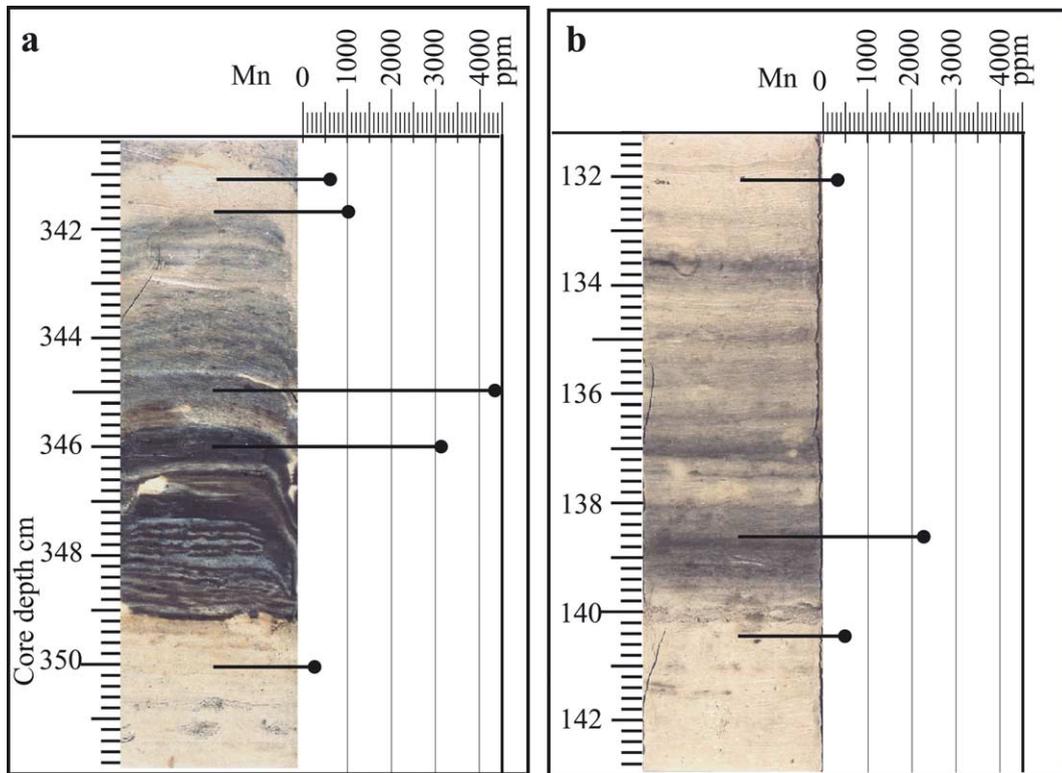

Fig. 10. Manganiferous silty clayey sequences in core KS 8813. Note the significant increase of Mn concentrations in these sequences. (a) Mn-sequence showing erosional surfaces and very black and Mn-rich layers. (b) Mn-sequences showing more diffuse black laminations.

and Fe vertical migration in the core towards a redox front, as observed frequently in very surficial Holocene deep-sea sediments when low deposition occurs (Damuth, 1977; McGeary and Damuth, 1973; Middleburg, 1993; Thomson et al., 1993; Weaver et al., 1989; Massé et al., 1996; Hyacinthe et al., 2001). Secondly, a contour current depositional process origin where the bottom circulation is sufficiently active to allow bio–physico–chemical sedimentation and direct precipitation of metallic oxides on the seafloor. That was already observed in the Quaternary sediments on the South Brazilian lower rise and abyssal plain (Massé, 1993; Viana, 1998), and elsewhere in the deep ocean when the deposition occurs far from the continental sources, below the CCD and under sluggish currents (Aplin and Cronan, 1985; Allouc, 1990; Kuhn et al., 1996).

The contour current origin of the Sao Tomé Mn-sequences fits the erosional contacts associated with these beds. The diagenetic origin that needs also low sedimentation rates between the turbidity current discharges, could be related either to periods of low hemipelagic–pelagic supply or to episodes of contour current activity, high enough to slow down the particle deposition. The supply variations should not play a major role as the Mn-sequences are observed interbedded with hemipelagic or pelagic deposits, and in a few cases, in the top of muddy turbidite sequences. Consequently, we suspect that the bottom current winnowing could be responsible for the low sedimentation rates in case of a diagenetic origin. That is why, whatever the origin, the Mn-sequences are here interpreted as the sedimentary record of contour current activity. It does not mean that the currents were strongly reinforced at the time of sequence deposition; only turbidity currents of less energy or lower frequency, may have made more effective the contour current impact on the sedimentation.

6. Sediment distribution

Detailed core analyses combined with the echofacies data make it possible to define the depositional facies and sequences, as well as their distribution according to the various environments defined above. In order to compare the lithology of each of the cores, we present a table of some lithologic and grain size parameters (Table 2).

6.1. Guanabara channel deposits

The Guanabara channel seafloor (Fig. 5) is characterized by a prolonged echo (IIB), or a more or less prolonged echo, with tiny discontinuous subbottom reflectors (IIA and IIA–IB) that suggest high-energy processes of sediment transport and deposition.

Sediments from core 11 (Fig. 11; Table 2), located in the deepest part of the channel (3650 m; Figs. 3a, 4b and 5c), have the thickest (up to 30 cm) and coarsest-grained silty–sandy basal turbidite layers (mean diameter 53 μm, exceptionally up to 140 μm with a mode of 410 μm), and the thickest debris-flows (a few decimeters) observed in the study area. They are interbedded in hemipelagite layers. Debris-flow deposits and turbidites represent 35% of the entire deposit. Pebbles of various size, composition and age are shown by 20%. Some of them correspond to white chalk, and are Eocene in age from the nannoflore (J. Giraudeau, pers. commun., 2001) and the monospecific planktonic foraminifera observed (J.-C. Pujol, pers. commun., 2001); they probably come from the nearby beds outcropping along SPPE. Ten of the turbidite sequences are of T1 type, and two of T2 type. One of the two is of T2-tr type (30 cm of silty sands) and deposited by fairly high-density turbidity currents.

6.2. Western flank and top of the levee

The western flank and the top of the levee mostly presents a distinct to semi-prolonged echo with numerous continuous to semicontinuous subbottom reflectors (IIA–IB).

Core 15 (Fig. 11; Table 2), located close to the channel core 11, is collected on the western flank of the levee (3590 m), where the levee crest is the lowest (Figs. 3a, 4b and 5c). It consists of major silty–clayey muds (hemipelagic muds 63%; pelagic muds 19%), and minor silty sands (18%). The

Table 2
Sediment facies and sequences in the collected cores

Facies and sequences			Guanabara channel	Levee			Transitional zone		
			KS 8811 3650 m	KS 8815 3590 m	KS 8812 3580 m	KS 8813 3636 m	KS 8814 3660 m	KS 8817 3834 m	KS 8816 3530 m
1	Calcareous muds	%		19	18	25	22	17	62
2	Mini–Maxi carbonate	%		< 5–50	< 5–60	< 5–55	< 5–50	< 5–55	10–70
3	Muds	%	65	63	71	69	53	65	38
4	Silts–sands	%	15	18	10	6	23	17	0
5	Silts–sands/muds	%	17	22	11	6	29	20	0
6	s+S layers > 5	cm	3	6	5	0	6	4	0
7	s+S layers > 10	cm	3	2	1	0	2	3	0
8	T. frequency	T/m	2.6	4.9	4.9	4.8	5	6.3	0
9	Turbidite sequence	%	15	28	32	24	44	38	0
10	Maximum mean diameter	μm	140	74	45	43	59	55	15
11	T1/T2	nb	10/2	20/8	25/5	34/4	17/6	29/7	0
12	T2/T2-tr	nb	2/1	8/5	5/4	4/0	6/2	7/5	0
13	Debris-flow or slump	%	20	1.5	0	1.5	0	0	0
14	Mn sequence	%	0	0	1	5	1.7	4	1.5
15	Foram-rich sequence	%	0	0	1	1.5	0	0	0

Legend: (1) Calcareous muds % is the pelagic sequence percentage for the entire deposit. (2) Mini–Maxi carbonate percemtage: minimum–maximum carbonate % observed in the muds. (3) Muds % is the percentage of hemipelagic sequences+upper silty clayey divisions (3 and 4) of T1 and T2 turbidite sequences. (4) Silts–sands % is the percentage of the silty–sandy layers (basal division of T1 and T2 turbidite sequences). (5) Silts–sands/muds is the silt–sand/mud ratio. (6) s+S layers > 5 cm is the number of silty–sandy basal turbidite division thicker than 5 cm. (7) s+S layers > 10 cm is the same but thicker than 10 cm. (8) T. frequency, T/m is the frequency of turbidite sequences per meter. (9) Turbidite sequence % is the percentage of the turbiditic deposits (T1+T2) with respect to the entire deposit. (10) Maximum mean diameter is the maximum mean diameter in μm observed in silty–sandy basal turbidite division (T1 or T2). (11,12) T1/T2 nb and T2/T2-tr nb are the number of sequence ratios. (13) Debris-flow or slump % is the debris-flow or slump percentage of the entire deposit. (14) Mn sequence % is the Mn sequence percentage of the whole deposits. (15) Foram-rich sequence % is the foraminifera sequence percentage of the entire deposit.

turbidite frequency is about 5/m. Six silty–sandy turbidite layers are thicker than 5 cm, and two of them thicker than 10 cm. They show the coarsest material observed on the levee (mean diameter up to 74 μm). The T1 sequences (20 T1, predominantly of T1a types) are the most frequent with respect to the T2 sequences (8 T2) and represent 15% and 13% of the entire deposit, respectively. Disturbed sediments at the top of the core suggest debris-flow deposits (1.5%). No Mn- and F-sequences are observed.

Core 12 (Fig. 11; Table 2), located on top of the levee (Figs. 3a, 4a and 5b), in a northern slightly shallower position (3580 m) than core 15, is composed of still more abundant muds (71%) and calcareous muds (18%), with minor silty sand turbidite layers (silt+sand/mud = 11%) than in core 15 (silt+sand/mud = 22%). Only five silty–sandy layers are thicker than 5 cm, with only

one thicker than 10 cm, and the maximum mean diameter is up to 45 μm. The turbidite frequency is similar (5/m) but it is lower for the upper 3.5 m of the core (4.3/m) than downcore (6.3/m). The T1 turbidites are still more abundant and represent 29% of all the deposits with rare T1b and T1–l (9%), while the T2 sequences, mostly of T2-tr type, number 3% only. One F-sequence, interbedded in hemipelagic–pelagic deposits, is observed at 2.75 m, and one Mn-sequence at the core top.

Both cores show that the levee top represents a fairly low energy environment subjected to predominant turbidity currents and hemipelagic–pelagic sedimentation. However, in the deepest part of the levee (core 15), the sandy turbidite beds have a slightly higher grain size and thickness, and a greater silt–sand/clay ratio. It suggests that the overflowing turbidity currents could be

KS 8811   KS 8815   KS 8812   KS 8813   KS 8814   KS 8817   KS 8816

Legend:

- ✳ Mn traces
- ✳✳✳✳✳ Mn -seq
- ■ T1
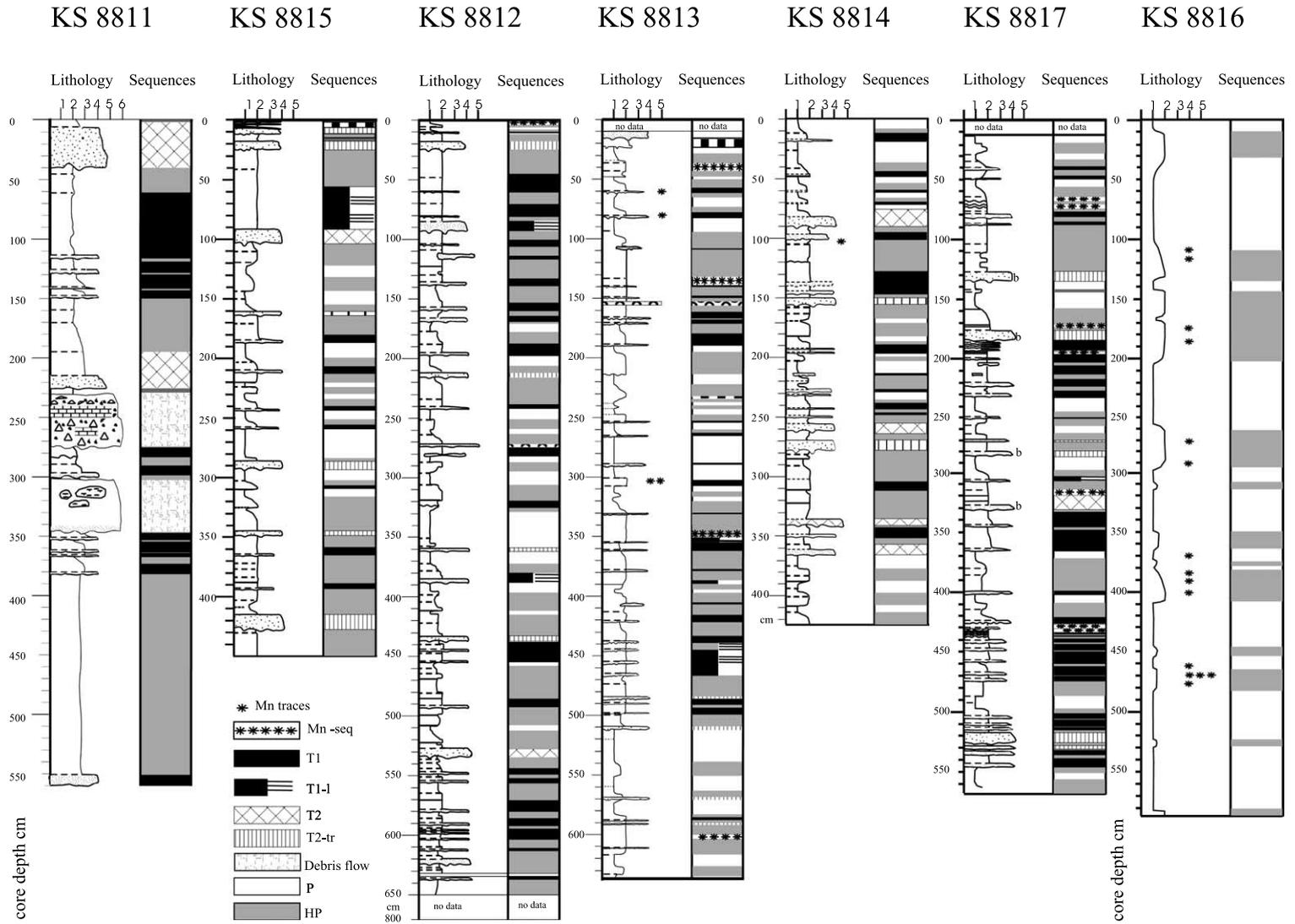- ■≡ T1-l
- ⊠ T2
- ▥ T2-tr
- Debris flow
- □ P
- ▨ HP

Fig. 11. Core lithology and sedimentary sequence interpretation (see text for explanation of facies).

of slightly higher density and velocity compared to the northern more elevated part (core 12): the higher the relief, the lower the energy of the currents.

6.3. Eastern flank of the levee

In the northern and central parts of the levee, IIA–IB echofacies is also predominant, and is associated with still more fine-grained sediments (core 13; Fig. 11; Table 2).

Core 13 was collected from the eastern flank of the levee (Figs. 3a, 4a and 5b), in the central area (3635 m). The muds (69%) and carbonate muds (25%) are very abundant with a very low silt+sand/mud ratio (6%). The turbidite frequency is similar to that of cores 15 and 12; as for core 12, it is slightly lower for the upper 3.5 m of the core, suggesting that most of the same turbidity currents flow over both areas. But the silty–sandy turbidite layers are thinner (no layers thicker than 5 cm), and the mean diameter never exceeds 43 μm. The T1 turbidites are still the most frequent, but with only 22% of all deposits. The T2-tr type accounts only for 2%. There are five Mn-sequences scattered throughout, and one F-sequence is present at 1.5 m below seafloor. Deformed deposits (1.5%, slump?) are observed at the top of the core.

6.4. Transitional zone

In the transitional zone, the surficial deposits of the central depression present a predominant distinct to semi-prolonged echo with subbottom reflectors (IIA–IB). This echo merges downslope into a very irregular seafloor surface, showing small-scale reliefs and depressions or mini-channels (core 14). Such patterns become more and more developed southward where they are associated with major hyperbolic echofacies (Fig. 8): either irregularly undulating echo (IIIB, core 17), interpreted as mudwaves and/or compressional ridges, or irregularly elevated hyperbolae without subbottom reflectors (IIIC), interpreted as strongly deformed deposits (hummocky bedforms and compressional ridges).

Core 14 (Fig. 11; Table 2) is located near the axis of the central depression in a thalweg (3660 m) that seems to transport the sediment from south to north (Figs. 3a and 4b). The core consists of major muds (53%) and carbonate muds (22%,), and minor silty sand layers (23%). It shows the upper silt+sand/mud ratio (29%) observed in the surveyed area. The turbidite frequency is similar to that of the levee cores (5/m). However, the silty sand layers are fairly thick with six layers thicker than 5 cm, two among them thicker than 10 cm, and with a mean diameter up to 59 μm. The T1 sequences are the most frequent (30%), with no sequences of T1-b or T1-l type. The T2 sequences (6 T2) represent 14% of the deposits, and two of them are of T2-tr type. There is only one layer with Mn traces and no F-sequence.

Core 17 (Figs. 3a and 11; Table 2) is located on the southeastern part of the central depression (3834 m), in an area with irregular wavy bedforms. The core contains major muds (65%) and carbonate muds (17%), fewer silty sand layers (17%) than core 14, and lower silty sand/mud ratio (20%). The turbidite frequency is the highest observed in the study area (6.3/m). However, the silty–sandy layers are fairly thin; four are thicker than 5 cm, and three among them are thicker than 10 cm, with a mean diameter up to 55 μm. As for core 14, the T1 sequences constitute a large part of the deposits (29%), with rare occurrence of sequences T1-b (6%) or T1-l (2%) types. The T2 sequences represent 9% of the deposits, and are mostly of T2-tr type. There are five Mn-sequences scattered throughout, and no F-sequence. Core 16 (Figs. 3a, 4d and 11; Table 2), is collected close to the Carioca channel, in the southernmost distal part of the system (3530 m), where the seafloor shows chaotic pattern (IIIC echo). The core almost totally consists of pelagic (62% of carbonate muds) and hemipelagic (38% of silty–clayey muds) deposits. There are no turbidite deposits. One Mn-sequence is observed, and numerous traces of Mn are scattered throughout the core.

Cores 14 and 17 in the transitional area reveal deposits that are fairly similar to the deposits on the levee, but the turbidite grain size and the silty sand/mud ratio may reach higher values. This suggests supply transported by other channels

than the Guanabara channel since the transitional zone displays a distal position with respect to the Guanabara channel overflowing turbidity currents, and should present finer-grained deposits. The sediment could probably come from the south through secondary channels supplied by the Carioca channel.

7. Discussion: sedimentary process, sediment distribution and origin

The main sedimentary processes that are involved in the deposition of the Upper Quaternary sediment of the Sao Tomé system are hemipelagic and pelagic processes, together with turbidity current processes. The role of the contour currents is difficult to assess as no typical contourite facies, as originally defined by Stow (1982), Faugères et al. (1984) and Gonthier et al. (1984), has been observed in the deposits.

The turbidite deposits occur in the form of fine-grained thin sequences that represent up to 44% of the entire deposits. The silty–sandy turbidite basal layers are never very thick (millimeters to centimeters usually, and exceptionally up to 3 dm). They correspond to turbidity currents of middle to very low energy that are directed by major or secondary channels, and flow over the channel levees into the adjacent overbank areas. Most of the levee turbidite deposits result from the Guanabara channel overflowing. In the southern and central part of this channel, a northward increase of the echo penetration (compare lines LA, BC, DE, FG, Figs. 4 and 5b–d) suggests a northward decreasing grain size, and south to north flowing turbidity currents. In the northernmost part of the channel, the echoes pass from a IIB echo (Figs. 5a and 6e) in the north, into a IIA then a IIA–IB1 echo (Figs. 5b–d and 8) southward, suggesting a north to south turbidity current trend and decreasing energy. If this is the case, there would be turbidity currents coming both from the northern and the southern sides. In the first case, the turbidity currents may be derived from the Carioca channel and have been probably initiated at the upper continental margin (Fig. 2, sector of the 'Sul Este', canyons, Viana, 1998). In the second case, they may have moved directly from the upper slope further north (sector of the Itapimiri and Almirante Camara canyons) through the Sao Paulo Plateau and the Macaé channel network. The turbidity currents flowing along the secondary channels may be derived directly from the Carioca channel or the Macaé channel, and also from the shallowest part of the Guanabara channel where the low relief of the levee would be conducive to overflow into the central depression.

Turbidite deposits are encountered in the entire system except for its southeasternmost part (core 16). The coarsest sediments are deposited in the Guanabara channel that acts as a trap for the turbidite and other debris-flow deposits, with only the fine-grained upper part of the turbidity currents overflowing the eastern channel levee. However, turbidites associated with the secondary channels are slightly coarser and more frequent than on the levee (compare cores 12 and 13 with cores 14 and 17, Table 2). This fits with sediments being mostly delivered into the secondary channels by direct transport from the Carioca channel (i.e. core 14), and probably also from the Macaé channel. Strong activity along the secondary channels is supported by erosional features visible in the 3.5-kHz profiles (Figs. 6f and 7b).

Whatever the current pathways, the deposited material has a continental origin as suggested by the abundance of quartz, feldspar and micas in the coarse-grained fraction, and kaolinite in the clay mineral assemblage. Significant proportions of planktic foraminifera in the coarse-grained fraction (20–40%) of turbidite basal layers suggest that the turbidity currents may have eroded pelagic-hemipelagic deposits on the slope where such deposits cover large areas (Massé et al., 1996; Viana and Faugères, 1998).

Hemipelagic and pelagic deposits form a veneer at the surface of the system or are interbedded into the turbidites. They may be deposited as hemipelagic–pelagic climatic sequences showing muds or slightly calcareous muds that pass gradually upward into calcareous muds. In some cases, hemipelagic mud may occur as individual layers with sharp basal and upper contacts. The deposition of such layers, together with foraminif-

era-rich layers and manganiferous sequences, may be interpreted as partly due to contour current activity.

The role of contour currents may be also investigated from the bedforms. Their role seems to be more important in the south of the system where depositional sediment waves cover the seafloor of the shallower part of the levee, and are interpreted to result from contour currents because of their very regular size and geometry. That interpretation is supported by core 16, located downslope of the sediment waves, which only consists of muds with variable carbonate contents, and is without any turbidites. Such an absence of turbidites may be explained by the core location, 350 m above the Carioca channel bottom, high enough to prevent the overflowing of concentrated turbidity currents. The only diluted currents that would reach the levee could then be pirated and the particles redistributed by the contour currents. Consequently, parts of what we have interpreted as hemipelagic deposits could be muddy contourites. Such processes may occur all over the system, but it is not clearly recorded by the deposits, probably because it is masked by the predominant gravity processes. Whatever the exact role of the contour currents, it remains minor in the system sedimentation.

Processes of reworking and post-depositional deformation by slides, slumps and debris-flows strongly affect the entire system and more particularly the transitional area. Those processes would be linked to a mobile Pliocene bed that has undergone diapiric processes, and would have formed the large-scale slide that caused the central depression, the material of which is partly transported further down onto the lower rise and abyssal plain (Viana et al., in press). Whatever their origin, most of the bedforms have been interpreted as hummocky structures, wavy irregular bedforms and compressional ridges. In addition, mass-flow processes in the form of debris-flows only occur significantly in the Guanabara channel. They may have been iniated along the SPPE as the Eocene reworked material, observed in the Guanabara channel deposits, may have come from the upper SPP Cretaceous–Paleocene series that probably outcrops along the escarpment.

In such a sedimentary process context, it is difficult to explain the trend of the entire system, and more especially of the Guanabara channel and some secondary channels that are parallel to the margin contours. From our data only, we may suggest that some of these channels may have been initiated as large-scale slope failures, eroded later by the currents, and used today as sediment pathway. However, the NNE–SSW trend of the entire system may be tectonically controlled as it is located at the foot of the Sao Paulo Plateau escarpment that corresponds to the distal boundary of the thick Aptian salty bed. In addition, the faults involved in the South Brazilian Basin oceanic expansion, as well as the transitional crust subsidence, could be responsible for such a control (Schobbenhaus et al., 1984).

8. Conclusions

The 'Sao Tomé deep-sea channel levee system', is elongated N–S, parallel to the margin bathymetric contour at the foot of the Sao Paulo Plateau escarpment, on the upper rise of the South Brazilian Basin. Because of the occurrence of active contour currents in the region, it was first interpreted as a drift system. Detailed analyses of 3.5-kHz profiles and seven cores allow the establishment of a more detailed system physiography and deposit distribution. Such an approach makes it possible to demonstrate that turbidite and hemipelagic–pelagic processes are predominant for the Upper Quaternary sediment deposition.

In the major channel the turbidites show the coarsest material collected in the study area, that never exceeds the fine sand grain size. They are associated with debris-flow deposits. Both deposits represent 15% and 20% of all the deposits, respectively. Turbidites on the levee and the transitional area towards the deeper rise are finer-grained with a thin silty–sandy basal layer and muddy upper divisions. They are frequently interbedded with the hemipelagic–pelagic muds (5 to 6 turbidites/m) and account for 24–44% of all the deposits. They result from turbidity currents overflowing from the major channel or from second-

ary channels that cross the system. The siliciclastic sediments have a continental origin, as shown by the component mineralogy. They are transported on the system via two channels that are located one in the north and the other one in the south of the system, and that feed both N–S and S–N directed turbidity currents. The silty sand/mud ratio evaluated for each core reaches values up to 29%. This suggests significant hydrocarbon reservoir potentiality for the system.

Post-depositional sediment deformations in the form of slides and slumps mostly affect the distal transitional area where they are responsible for most of the bedforms such as hummocky structures, wavy bedforms, compressional ridges, and diapir-like structures.

There is only slight evidence for contour current activity recorded by the depositional geometry, bedforms and facies. A field of sediment waves, located in the southern part of the system, has been interpreted as deposited by these currents. Part of the erosion observed in the secondary channels that have a trend parallel to the margin could also be due to the current activity. However, no typical contourite facies as those described in the literature have been observed. The only features that could be interpreted as contourites are manganiferous-rich layers and some other deposits like top-truncated sequences or sandy foraminifera layers. That means that the contour currents only play a minor role in the depositional processes, though a major contour current controlled sedimentation was suggested by the hydrological background and the system trend.

Our results indicate that we have to be cautious when interpreting the depositional processes of deep-sea levee. Only an approach combining acoustic data analyses with detailed analyses of core lithology, especially of the thin sandy-silty layers, and the Mn-rich muddy layers, seems today the most reliable way to discriminate deep-sea depositional processes.

Acknowledgements

References

Allouc, J., 1990. Quaternary crusts on slopes of the Mediterranean sea: A tentative explanation for their genesis. Mar. Geol. 94, 205–206.

Alvés, R.A., 1999. Estudo seismoestratigrafico do bacia do Brasil. Unpubl. M.Sc. Thesis, Universidade Federal Fluminense, Niteroi, RJ, 88 pp.

Aplin, A.C., Cronan, D.S., 1985. Ferromanganese oxide deposits from the Central Pacific Ocean, II. Nodules and associated sediments. Geochim. Cosmochim. Acta 49, 437–451.

Biscaye, P., 1965. Mineralogy and sedimentation of recent deep-sea clay in the Atlantic ocean and adjacent seas and oceans. Geol. Soc. Am. Bull. 76, 803–832.

Brehme, I., 1984. Vales submarinos entre o banco dos Abrolhos e Cabo Frio. Unpubl. M.Sc. Thesis, Universidade Federal de Rio de Janeiro, Rio de Janeiro, 116 pp.

Castro, D.D., 1992. Morfologia da margem continental sulest-sul brasileira e estratigrafia sismica do sopé continental. Unpubl. M.Sc. Thesis, Universidade Federal de Rio de Janeiro, Rio de Janeiro, 226 pp.

Chamley, H., 1975. Influence des courants profonds au large du Brésil sur la sedimentation. 9° Congrès International Sédimentologie, Nice, pp. 13–19.

Damuth, J.E., 1977. Late Quaternary sedimentation in the western equatorial Atlantic. Geol. Soc. Am. Bull. 88, 695–710.

Damuth, J.E., 1980. Use of high-frequency (3.5–12 kHz) echograms in the study of near-bottom sedimentation processes in the deep-sea: A review. Mar. Geol. 38, 51–75.

Damuth, J.E., Hayes, D.E., 1977. Echocharacter of the east Brazilian continental margin and its relationship to sedimentary processes. Mar. Geol. 24, 73–95.

DeMadron, X.D., Weatherly, G., 1994. Circulation, transport and boundary layers of the deep currents in the Brazil Basin. J. Mar. Res. 52, 583–638.

Faugères, J.C., 1988. Mission océanographique Byblos. Bassin du Brésil. Géochronique, Société Géologique de France, Bureau de Recherches Géologiques et Minières 27, 8.

Faugères, J.C., Gonthier, E., Stow, D.A.V., 1984. Contourite drift molded by deep Mediterranean outflow. Geology 12, 296–300.

Faugères, J.C., Stow, D.A.V., Imbert, P., Viana, A., 1999. Seismic features diagnostic of contourite drifts. Mar. Geol. 162–1, 1–38.

Gamboa, L.A.P., Buffler, R.T., Barker, P.F., 1983. Seismic stratigraphy and geologic history of the Rio Grande Gap and Southern Brazil Basin. In: Biju-Duval, B., Moore,

J.C. et al. (Eds.), Initial Reports of the Deep Sea Drilling Project 72. US Government Printing Office, Washington, DC, pp. 481–498.

Gervais, A., Mulder, T., Savoye, B., Migeon, S., Cremer, M., 2001. Recent processes of levee formation on the Zaire deep-sea fan. Comptes Rendus de l'Académie des Sciences, Paris, IIA, 332 (6), pp. 371–378.

Gonthier, E., Faugères, J.C., Stow, D.A.V., 1984. Contourite facies of the Faro Drift, Gulf of Cadix. In: Stow, D.A.V., Piper, D.J.W. (Eds.), Fine-Grained Sediments: Deep Water Processes and Facies. Geological Society of London, Special Publication 15, pp. 275–292.

Gorini, M.A., Maldonado, P.R., Silva, C.G., Souza, E.A., Bastos, A.C., 1998. Evaluation of deep water submarine hazards at Campos Basin, Brazil. Offshore Technology Conference, Houston, TX, 1998, OTC 8644, pp. 133–141.

Hiscott, R.N., Hall, F.R., Pirmez, C., 1997. Turbidity-current overspill from the Amazon channel: Texture of the silt/sand load, paleoflow from anisotropy of magnetic susceptibility and implications for flow processes. Proceedings of the Ocean Drilling Program Scientific Results 155, pp. 53–78.

Hogg, N.G., Owens, W.B., Siedler, G., Zenk W., 1996. Circulation in the deep Brazil Basin. In: Wefer, G., Berger, W.H., Siedler, G., Webb, D.J. (Eds.), The South Atlantic: Present and Past Circulation. Springer, Berlin, pp. 13–44.

Hogg, N.G., Zenk, W., 1997. Long-period changes in the bottom water flowing through Vema channel. J. Geophys. Res. 102, 15639–15646.

Hyacinthe, C., Anschutz, P., Carbonnel, P., Jouanneau, J.M., Jorissen, F.J., 2001. Early diagenetic processes in the muddy sediments on the Bay of Biscay. Mar. Geol. 177, 111–128.

Jacobi, R.D., 1982. Microphysiography of the southeastern north Atlantic and its implications for the distribution of near-bottom processes and related sedimentary facies. Bulletin Institut Géologie Bassin d'Aquitaine, Bordeaux, 31–32, pp. 31–46.

Kuhn, T., Halbach, P., Maggiulli, M., 1996. Formation of ferromanganese microcrusts in relation to glacial/interglacial stages in Pleistocene sediments from Ampere Seamount (Subtropical NE Atlantic). Chem. Geol. 130, 217–232.

Latouche, C., Maillet, N., 1984. Evolution of Cenozoïc clay assemblages in the Barbados ridge. In: Biju-Duval, B., Moore, J.C., et al. (Eds.), Deep Sea Drilling Project: Sites 541, 542 and 543. Initial Reports of the Deep Sea Drilling Project 78, US Government Printing Office, Washington, DC, pp. 343–356.

McCave, I.N., Tucholke, B.E., 1986. Deep current-controlled sedimentation in the western North Atlantic. In: Vogt, P.R., Tucholke, B.E. (Eds.), The Geology of North America: The Western North Atlantic Region, decade of North America Geology. Geological Society of America, Boulder, CO, pp. 451–468.

McGeary, D.F.R., Damuth, J.E., 1973. Postglacial iron-rich crusts in hemipelagic deep-sea sediment. Geol. Soc. Am. Bull. 84, 1201–1212.

Machado, L.C.R., Kowsmann, R.O., Almeida, J.R., Murakami, C.Y., Schreiner, S., Miller, D.J., Piauilino, P.O., 1997.

Geometria da porçao proximal do sistema deposicional turbiditeo pleistocenico da formaçao Carpebus, Bacia de Campos. Modelo para heterogeneidade de reservatorio. I Simposio sobre Turbiditos. PETROBRAS/SEREC/CENSUD, Rio de Janeiro, pp. 104–110.

Massé, L., 1993. Sédimentation océanique profonde au Quaternaire. Flux sédimentés et paleocirculations dans l'Atlantique Sud-Ouest: Bassin Sud-Brésilien et prisme d'accrétion Sud-Barbade. Unpubl. Thèse Université Bordeaux I, 339 pp.

Massé, L., Faugères, J.C., Bernat, M., Pujos, A., Mezerais, M.L., 1994. A 600,000 year record of Antarctic Bottom Water activity inferred from sediment textures and structures in a sediment core from the Southern Brazil Basin. Paleoceanography 9–6, 1017–1026.

Massé, L., Faugères, J.C., Pujol, C., Pujos, A., Labeyrie, L.D., Bernat, M., 1996. Sediment flux distribution in the Southern Brazil Basin during the late Quaternary. The role of deep-sea currents. Sedimentology 43, 115–132.

Mello, G.A., 1988. Processos sedimentares recentes na bacia do Brazil: Setor sudeste-sul. Unpubl. M.Sc. Thesis, Universidade Federal de Rio de Janeiro, Rio de Janeiro, 169 pp.

Mello, G.A., Flood R.D., Orsi, T.H., Lowrie, A., 1992. Southern Brazil basin: Sedimentary processes and features for continental rise evolution. In: Poag, C.V., Graciansky, J. (Ed.), Geologic Evolution of Atlantic Continental Rise. Van Nostrand Reinhold, New York, pp. 189–213.

Mézerais, M.L., Faugères, J.C., Figueiredo, A.L., Massé, L., 1993. Contour current accumulation off Vema channel mouth Southern Brazil basin. Sediment. Geol. 82, 173–188.

Middleburg, J.J., 1993. Turbidites provide a unique opportunity to study diagenetic processes. Geol. Mijnb. 72, 15–21.

Migeon, S., Weber, O., Faugères, J.C., Saint Paul, J., 1999. SCOPIX: A new X-ray imaging system for core analysis. Geo-Mar. Lett. 18, 251–255.

Migeon, S., Savoye, B., Zanella, E., Mulder, T., Faugères, J.C., Weber, O., 2001. Detailed seismic-reflection and sedimentary study of turbidite sediment waves on the Var Sedimentary Ridge (SE France): Significance for sediment transport and deposition and for the mechanisms of sediment-wave construction. Mar. Pet. Geol. 18, 179–208.

Miller, D.J., Kowsmann, R.O., Rizzo, J.G., 1996. Feiçoes fisiograficas da bacia de Campos à luz de novo dados batimétricos. In: Congres Brasil Geologia 39, Annales Salvador, SBG, 3, pp. 397–398.

Muller, T.J., Ikeda, Y., Nonato, L.V., 1997. Direct current measurements of western boundary currents off Brasil between 20°S and 28°S, WOCE South Atlantic. Workshop, Brest, Livre de Résumés.

Petchick, R., Kuhn, G., Gingele, F., 1996. Clay mineral distribution in surface sediment in the South Atlantic: Sources, transport and relation to oceanography. Mar. Geol. 130, 203–229.

Reid, J.L., Nowlin, W.D., Patzert, W.C., 1977. On the characteristics and circulation of the southwestern Atlantic Ocean. J. Phys. Oceanogr. 7, 62–91.

Reid, J.L., 1989. On the total geostrophic circulation in the

South Atlantic Ocean: Flow, patterns, tracers, and transports. Prog. Oceanogr. 23, 149–244.

Reid, J.L., 1996. On the circulation in the South Atlantic ocean. In: Wefer, G., Berger, W.H., Siedler, G., Webb, D.J. (Eds.), The South Atlantic: Present and Past Circulation. Springer, Berlin, pp. 13–44.

Schobbenhaus, C., De Almeida Campos, D., Derze, G.R., Asmus, H.E., 1984. Geologia do Brasil. Departamento Nacional da Produçao Mineral, Ediçao Comemorativa do Cinqüentenario, 501 pp.

Siedler, G., Müller, T.J., Onken, R., Arhan, M., Mercier, H., King, B.A., Saunders, P.M., 1996. The Zonal WOCE Sections in the South Atlantic. In: Wefer, G., Berger, W.H., Siedler, G., Webb, D.J. (Eds.), The South Atlantic: Present and Past Circulation. Springer, Berlin, pp. 83–104.

Stow, D.A.V., 1982. Bottom currents and contourites in the North Atlantic. Bull. Inst. Geol. Bassin d'Aquitaine, Bordeaux 31, 151–166.

Thomson, J., Jarvis, I., Green, D.R.H., Green, D.A., Clayton, T., 1993. Mobility and immobility of redox-sensitive elements in deep-sea turbidites during shallow burial. Geochim. Cosmochim. Acta 2–4, 643–656.

Viana, A.R., 1998. Le rôle et l'enregistrement des courants océaniques dans les dépôts de marges continentales: la marge du bassin sud-est Brésilien. Unpubl. Ph.D Thesis, Université de Bordeaux I, 364 pp.

Viana, A.R., Faugères, J.C., 1998. Upper slope sand deposits: The example of Campos Basin, a latest Pleistocene/Holocene record of the interaction between along and across slope currents. In: Stoker, M.S., Evans, D., Cramp, A. (Eds.), Geological Processes on Continental Margins: Sedimentation, Mass-Wasting and Stability. Geological Society of London, Special Publication 129, pp. 287–316.

Viana, A.R., Figueiredo, A., Faugères, J.C., Lima, A., Gonthier, E., Brehme, I., Zaragosi, S., 2003. The Sao Tome deepsea turbidite system (South Brazilian Basin): Cenozoïc seismic stratigraphy and sedimentary processes. AAPG Bull. 87 (5), 873–874.

Weaver, P.P.E., Thomson, J., Jarvis, I., 1989. The geology and geochemistry of Madeira Abyssal Plain sediments: A review. In: Freeman, T.J. (Ed.), Advances in Underwater Technology, Ocean Science and Offshore Engineering. Society for Underwater Technology, Graham and Trotman, pp. 51–78.